Machine learning-based signature for prognosis and drug sensitivity in hepatocellular carcinoma using glycolysis-related gene

YUFAN ZHOU[1], WEI LIU[1], ZHIXUE FANG[1], KE ZHOU[1], XING HUANG[1], SHANZHENG LU[1], WEILIN ZHANG[1], QIAOCHENG WEN[1], XU CHEN[2] and ZHIGANG XIAO[1]

[1]Department of General Surgery, Hunan Provincial People's Hospital, The First Affiliated Hospital of Hunan Normal University, Changsha, Hunan 410005, P.R. China; [2]Department of Hepatobiliary Surgery, Hunan Provincial People's Hospital, The First Affiliated Hospital of Hunan Normal University, Changsha, Hunan 410005, P.R. China

Received May 9, 2025; Accepted September 23, 2025

DOI: 10.3892/ol.2025.15384

Abstract. Hepatocellular carcinoma (HCC) is one of the most prevalent tumors in the world and poses a considerable threat to global healthcare. The reprogramming of glucose metabolism in tumor cells has demonstrated a notable association with the genesis, advancement and resistance to the chemotherapy of malignancies. In the present study, 10 integrative machine learning algorithms were used to develop a glycolysis-related signature (GRS) using four datasets. Several predictive approaches were used to evaluate the performance of GRS in predicting the immunology response. In addition, *in vitro* experiments were performed to explore the biological functions of monocarboxylic acid transporter 1 (MCT1) in HCC. The optimal GRS developed by the Least Absolute Shrinkage and Selection Operator algorithm served as a risk factor for patients with HCC. Patients with HCC and a high-risk score experienced a poor prognosis, with the area under the curves of 1, 3 and 5-year receiver operating characteristic curves being 0.777, 0.787 and 0.766, respectively. A low-risk score indicated higher levels of $CD8^+$ cytotoxic T cells and M1 macrophages, as well as an increased estimation of stromal and immune cells in malignant tumors score. Moreover, increased tumor mutational burden score and programmed cell death protein 1 and cytotoxic T-lymphocyte-associated protein 4 immunophenoscores, as well as decreased Tumor Immune Dysfunction and Exclusion and tumor escape scores were found in patients with HCC that had low-risk scores. The IC_{50} values of docetaxel, oxaliplatin, crizotinib and osimertinib were lower in HCC cases with a high-risk score. In addition, the gene set scores that were associated with angiogenesis and Notch signaling were higher in the high-risk score group. Downregulation of MCT1 inhibited the proliferation, migration and invasion of HCC cells and promoted the apoptosis of HCC cells. In conclusion, the present study developed a novel GRS for HCC, serving as an indicator for predicting clinical outcomes and responses to immunotherapy.

Correspondence to: Professor Zhigang Xiao, Department of General Surgery, Hunan Provincial People's Hospital, The First Affiliated Hospital of Hunan Normal University, 61 Jiefang West Road, Changsha, Hunan 410005, P.R. China
E-mail: xzgcsu@163.com

Professor Xu Chen, Department of Hepatobiliary Surgery, Hunan Provincial People's Hospital, The First Affiliated Hospital of Hunan Normal University, 61 Jiefang West Road, Changsha, Hunan 410005, P.R. China
E-mail: chenxu941218@163.com

Key words: glycolysis, machine learning, immunotherapy, hepatocellular carcinoma, prognostic signature

Introduction

Hepatocellular carcinoma (HCC) is a primary malignancy of the liver and remains one of the most lethal cancers worldwide (1). A previous study indicated that >900,000 new cases are diagnosed annually, with >830,000 mortalities attributed to HCC, underscoring its critical burden on global health systems (2). Due to the fact that HCC is typically discovered at an advanced stage, numerous patients are denied the chance to have surgery (3). Although a number of approaches are available for patients with HCC in addition to surgery, including percutaneous ablation, liver transplantation and immunotherapy, the clinical prognosis for patients with HCC remains unfavorable, as <20% survive beyond 5 years (3). The main factors contributing to the poor clinical outcomes in patients with HCC are high heterogeneity, invasiveness and metastatic potential (4). Additionally, reliable biomarkers for predicting prognosis and guiding personalized therapeutic decisions in HCC remain scarce.

An important function of tumor cells is metabolic reprogramming. The 'Warburg effect' refers to the concept that tumor cells utilize ~80% of glucose for ATP synthesis by aerobic glycolysis, which is also characterized by the production of lactic acid, even in the presence of adequate oxygen (5). This aberrant glucose metabolism not only sustains rapid cell proliferation but also serves pivotal roles in cancer

progression, metastasis and resistance to chemotherapy (6). Enhanced glycolytic activity has been identified as a hallmark of HCC, with multiple glycolysis-related genes (GRGs) having been implicated in its development and progression (7). By promoting glycolysis, a number of genes are involved in the progression of HCC (8). Numerous intracellular and extracellular proteins are susceptible to the effects of lactylation (9). In addition, histone lactylation is also involved in numerous processes, including macrophage polarization under hypoxic conditions and tumorigenesis (10).

Previous efforts have explored glycolysis-related signatures (GRS) as prognostic tools across various malignancies, including breast cancer (11), bladder cancer (12) and HCC (13). Due to the central role of glucose metabolism in tumor biology, identifying glycolysis-associated genes that predict patient outcomes and therapeutic responses could offer valuable insights into HCC management.

In the present study, transcriptomic data from The Cancer Genome Atlas (TCGA) was used to construct a 7-GRS using 10 integrative machine learning algorithms. In addition, immune scores and immune cell infiltration associated with the glycolysis-associated gene signatures were investigated. The present study aimed to fully explore the role of GRGs in the prognosis of patients with HCC.

Materials and methods

Data acquisition. TCGA (n=329; https://portal.gdc.cancer.gov/), GSE72094 (n=90) (14), ICGC (n=228; https://dcc.icgc.org/) and GSE14520 (n=218) (15) datasets provided the mRNA level data of HCC. The present study excluded metastatic HCC cases. The GSE91061 (melanoma; n=89) (16) and IMvigor210 (bladder cancer; n=298) (17) datasets were used to investigate the relationship between immunotherapy response and GRS. GRG lists (Table SI) were acquired from three studies (18-20) and hallmark gene sets of gene set enrichment analysis (GSEA).

Integrative machine learning algorithms constructed an optimal GRS. Differentially expressed genes (DEGs) were obtained using the R package 'limma' (version 4.2.1; RStudio, Inc.) (21), with a cut-off level of LogFC ≥2. Univariate Cox analysis was carried out to determine the potential prognostic biomarkers within GRGs. These potential biomarkers were then utilized to develop a stable prognostic GRS through integrative machine learning analysis. The process encompassed 10 machine learning techniques: i) Random survival forest; ii) survival support vector machine; iii) ridge; iv) elastic network; v) supervised principal components; vi) stepwise Cox; vii) generalized boosted regression modelling; viii) partial least squares regression for Cox; ix) CoxBoost; and x) Least Absolute Shrinkage and Selection Operator (LASSO). The regularization parameter λ in the LASSO models was determined through 10-fold cross-validation, while the tradeoff parameter α was set between 0 and 1 (interval=0.1). When α is equal to 1, LASSO is executed. The GRS was developed in the following four steps using R scripts (https://github.com/Zaoqu-Liu/IRLS) obtained from a previous study (22): i) In order to investigate prognostic biomarkers in TCGA dataset, univariate Cox regression was used; ii) after which, algorithm combinations were fitted to the prediction model of TCGA dataset; iii) all algorithm combinations were carried out in Gene Expression Omnibus cohorts; and iv) the C-index was computed for each cohort. After obtaining the GRS score of the patients with HCC, the R package 'survminer' (https://cran.r-project.org/web/packages/survminer/index.html) containing the 'surv_cutpoint' function was used to identify the optimal cut-off for separating patients with HCC into high and low GRS score groups. Using the R package 'rms' (https://cran.r-project.org/web/packages/rms/index.html), the C-index curves for prognostic signatures and clinical features were also determined. The prognosis of HCC was examined using univariate and multivariate Cox analyses to investigate potential risk factors. Based on GRS score and additional clinical factors, the R package 'nomogramEx' (https://cran.r-project.org/web/packages/nomogramEx/index.html) was used to construct a predicting nomogram.

Immune infiltration analysis. Estimation of stromal and immune cells in malignant tumors (ESTIMATE) score of patients with HCC was determined using ESTIMATE analysis (23). The R package 'Immunedeconv' (24), a tool that integrates six algorithms, was utilized to explore the association between immune cells and GRS scores. The single sample GSEA method was applied to evaluate the levels of immune cells and scores related to immune activities or functions. Additionally, the R package 'GSVA' (25) was used to calculate the scores for the 'h.all.v7.4.symbols.gmt' gene set (https://data.broadinstitute.org/gsea-msigdb/msigdb/release/7.4/).

Drug sensitivity analysis. GRS may predict the potential benefits of immunotherapy for patients with HCC and its ability to do this was examined through various prediction scores, such as the Tumor Immune Dysfunction and Exclusion (TIDE) score, immunophenoscore, tumor escape score and tumor mutational burden (TMB) score. Individuals with a lower TIDE score and a higher TMB score are more likely to respond positively to immunotherapy and have reduced chances of immune evasion. Subsequently, the IC_{50} values for each drug in each HCC case were determined using the R package 'oncoPredict' (26).

Cell culture. The human normal liver cell line (THLE-2) was maintained in bronchial epithelial cell growth medium (ScienCell Research Laboratories, Inc.) and HCC cell lines (MHCC97H, HCCLM3 and SNU449) were maintained in DMEM (Thermo Fisher Scientific, Inc.). The medium was supplemented with 10% fetal bovine serum (Biological Industries; Sartorius AG) and 1% penicillin/streptomycin. All cells were cultured in a humidity incubator with 5% CO_2 at 37˚C.

Western blotting. Total protein was extracted by lysing cells in RIPA buffer containing protease inhibitors (Soochow New Cell & Molecular Biotech Co., Ltd.). Protein concentration was determined using a BCA assay kit (Thermo Fisher Scientific, Inc.). Equal amounts proteins (40 μg/lane) were then separated by SDS-PAGE on a 12% gel (Soochow New Cell & Molecular Biotech Co., Ltd.), and further transferred onto PVDF membranes (Soochow New Cell & Molecular

Biotech Co., Ltd.). After blocking with 5% skimmed milk at room temperature for 2 h, the membranes were incubated overnight with specific primary antibodies at 4˚C. The membranes were detected using an ultra-sensitive ECL kit (Soochow New Cell & Molecular Biotech Co., Ltd.), and the grayscale values of the protein bands were analyzed using ImageJ 1.0 software (National Institutes of Health). The following antibodies were used: Anti-MCT1 (1:1,000; cat. no. 20139-1-AP; Proteintech Group, Inc.), anti-epithelial cadherin (E-cadherin; 1:1,000; cat. no. 3195; Cell Signaling Technology, Inc.), anti-neural cadherin (1:1,000; cat. no. 13116; Cell Signaling Technology, Inc.), with anti-GAPDH (1:2,000; cat. no. 5174; Cell Signaling Technology, Inc.) and anti-heat shock protein 90 (1:1,000; cat. no. 4784; Cell Signaling Technology, Inc.) used as the loading control.

Lentiviral transduction for MCT1 knockdown. MHCC-97H cells were transduced with MCT1-targeting lentivirus (Shanghai GeneChem Co., Ltd.) following the supplier's protocol. Puromycin selection (2 μg/ml) was applied 48 h post-transduction to establish stable knockdown clones. In the maintenance phase, MHCC-97H cells were cultured in medium containing puromycin (0.5 μg/ml). After cells were cultured for 7-10 days, subsequent experiments were continued. Knockdown efficiency was demonstrated through western blotting. The short hairpin RNA (shRNA) sequences were as follows: shRNA1 sense, 5'-GCTCCGTATTGTTTG AAACAT-3'; anti-sense, 5'-ATGTTTCAAACAATACGG AGC-3'; shRNA2 sense, 5'-GCAGGGAAAGATAAGTCT AAA-3'; anti-sense, 5'-TTTAGACTTATCTTTCCCTGC-3'; short hairpin control sense, 5'-TTCTCCGAACGTGTCACG T-3'; anti-sense, 5'-ACGTGACACGTTCGGAGAA-3'.

Colony formation assay. A total of 500 MHCC-97H cells were plated in each well of a 6-well plate and incubated for 2 weeks in a humidity incubator with 5% CO_2 at 37˚C. After removing culture medium, the cells were fixed with 100% methanol at room temperature for 20 min, and stained by 0.1% crystal violet (Beyotime Biotechnology) at room temperature for 30 min. Finally, the colonies defined as clusters containing >50 cells were counted under a light microscope.

Flow cytometry. Flow cytometry was performed using a CytoFLEX™ flow cytometer (Beckman Coulter, Inc.). For cell cycle analysis, MHCC-97H cells were fixed with 70% ethanol at -20˚C overnight, and stained with 5 μg/ml PI (MultiSciences Biotech Co., Ltd.) at room temperature in the dark for 30 min. The cycle distribution of cells was analyzed using CytExpert 2.0 software (Beckman Coulter, Inc.). The cell apoptosis was detected using the Annexin V-FITC apoptosis assay kit (MultiSciences Biotech Co., Ltd.) according to the manufacturer's instructions. Cell apoptosis rate was analyzed using CytExpert 2.0 software (Beckman Coulter, Inc.).

Wound-healing assays. Cell migration was evaluated using a wound healing assay. A total of $5x10^5$ MHCC-97H cells were cultured in each well of a 6-well plate until they reached ~90% confluency in a humidified incubator with 5% CO_2 at 37˚C. Confluent monolayers in 6-well plates were scratched with a 100 μl pipette tip, and the medium was replaced with a complete medium containing 1% FBS (Biological Industries; Sartorius AG). At the time points of 0 h and 24 h, the gap distances after the wound were captured by a light microscopy (magnification, x10; Olympus Corporation). The cell migration rate was calculated using the following formula: Cell migration rate (%)=[(width at 0 h-width at 24 h)/width at 0 h] x100%.

Transwell assay. Invasion was assessed using Matrigel-coated Transwell chambers (Corning, Inc.). Matrigel (BD Biosciences) was diluted with PBS buffer (1:8) at 4˚C, with 100 μl evenly precoated on the surface of polycarbonate membrane in upper chamber at 37˚C for 2 h. A total of $5x10^4$ MHCC-97H cells were seeded in the upper chamber with serum-free medium and 500 μl complete medium containing 10% FBS (Biological Industries; Sartorius AG) was added to the lower chamber. The cells were cultured in a humidity incubator with 5% CO_2 at 37˚C for 24 h. Then the cells invaded to bottom membrane of chamber were fixed with 4% paraformaldehyde for 30 min and stained with 0.1% crystal violet (Beyotime Biotechnology) at room temperature. A total of five fields of vision were randomly selected and counted under an inverted microscope (magnification, x50; Olympus Corporation).

Statistical analysis All statistical analyses were conducted using R software and GraphPad Prism (version 9.2.0; Dotmatics). All results represent the mean ± standard deviation of assays performed at least three independent experiments. A two-sided unpaired Student's t-test was used for intergroup comparison, while a one-way ANOVA with a Tukey's post-hoc test was used for comparisons between multiple groups. The relationships between two continuous variables were assessed through Pearson correlation analysis. To compare differences in Kaplan-Meier survival curves, the two-sided log-rank test was applied. $P<0.05$ was considered to indicate a statistically significant difference.

Results

Integrative machine learning algorithms develop an optimal prognostic GRS. Using LogFC ≥2 as the cut-off, 2,898 DEGs in total were obtained in HCC (Fig. S1A) and 215 differentially expressed GRGs were identified among these DEGs (Fig. S1B). A total of 80 differentially expressed GRGs were shown to have a significant association with the prognosis of patients with HCC according to Cox univariate analysis (Fig. S1C; $P<0.05$). Using 10 machine learning-based methods, 30 different types of prognostic models were developed (Fig. 1A) and the C-index for each prognostic model was determined. The model built using the LASSO approach achieved the highest mean C-index of 0.78 and was selected as the final signature. This final GRS comprised the following seven genes: Treacle ribosome biogenesis factor 1 (TCOF1), replication factor C subunit 4 (RFC4), ribonucleic acid export 1 (RAE1), kinesin family member 2C (KIF2C), DEP domain containing 1 (DEPDC1), activity dependent neuroprotector homeobox (ADNP) and MCT1. The risk score was calculated using the following formula: Risk score=(-0.0825 x $TCOF1^{expression}$) + (0.0254 x $RFC4^{expression}$) + (0.1454 x $RAE1^{expression}$)+(0.0158x$KIF2C^{expression}$)+(0.1254x$DEPDC1^{expression}$)+

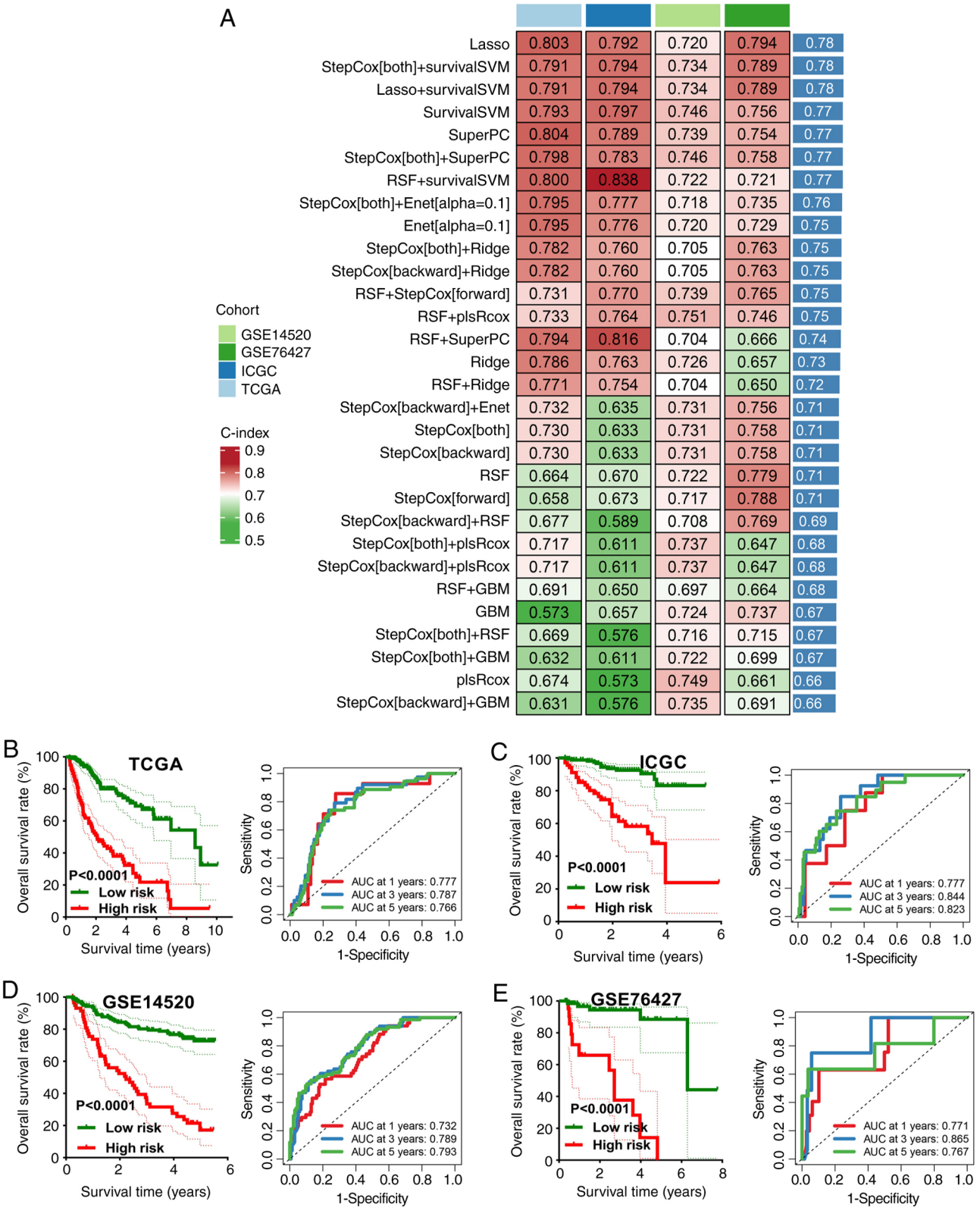

Figure 1. Construction and validation of the GRS. (A) C-index values of prognostic models developed using 10 different machine learning algorithms in training and validation datasets. Kaplan-Meier survival curves and corresponding time-dependent receiver operating characteristic curves for patients with high vs. low GRS in (B) TCGA, (C) ICGC, (D) GSE14520 and (E) GSE76427 cohorts. GRS, glycolysis-related signature; TCGA, The Cancer Genome Atlas; ICGC, International Cancer Genome Consortium; AUC, area under the curve.

(0.0354 x ADNP ^{expression}) + (0.768 x MCT1 ^{expression}). HCC cases were divided into high-risk and low-risk categories using the optimal cut-off. The results showed 1, 3 and 5-year area under the curves (AUCs) of 0.777, 0.787 and 0.766 in TCGA cohort; 0.777, 0.844 and 0.823 in the ICGC cohort; 0.732, 0.789 and 0.793 in the GSE14520 cohort and 0.771, 0.865 and 0.767 in the

GSE76427 cohort. Furthermore, a poor overall survival (OS) rate was found in patients with HCC with a high-risk score in TCGA, ICGC, GSE14520 and GSE76427 cohorts (all P<0.001; Fig. 1B-E).

Evaluation of the performance of GRS. Multivariate and univariate Cox regression analyses demonstrated that GRS was an independent prognostic factor across all four datasets (all P<0.05; Fig. 2A and B). When compared with conventional clinical features such as age, sex and tumor stage, the GRS-based risk score achieved superior prognostic discrimination as reflected by its higher C-index value (Fig. 2C-F). Notably, among 31 existing HCC prognostic signatures, GRS outperformed all others with regards to the C-index value (Table SII; Fig. 2G).

A predictive nomogram was also constructed incorporating the GRS and clinical variables to estimate 1, 3 and 5-year survival probabilities (Fig. 2H). Calibration plots consistency between predicted and observed outcomes (Fig. 2I), further validating the clinical utility of the model.

GRS-based distinct immune microenvironment in HCC. Immune microenvironment analysis revealed notable correlations between GRS and immune cell infiltration. Risk scores were positively or negatively associated with specific immune populations, including $CD8^+$ T cells, M1 and M2 macrophages (Fig. 3A-D). Patients in the low-risk group showed elevated levels of immune-activated cell types, including B cells, natural killer cells, neutrophils, tumor-infiltrating lymphocytes and $CD8^+$ T cells, compared with the high-risk group (Fig. 3E). Moreover, patients in the low-risk group also demonstrated higher enrichment scores in immune-related functions such as antigen-presenting cell co-stimulation, cytolytic activity, human leukocyte antigen (HLA) molecule expression, inflammation promotion and T cell co-stimulation (Fig. 3F). Additionally, stromal score, immune score and ESTIMATE scores were significantly higher in the low-risk group compared with the high-risk group, indicating a more active and immunologically enriched tumor microenvironment (TME; Fig. 3G-I; all P<0.05).

GRS acts as an indicator for drug sensitivity in HCC. Predictive efficacy of the GRS-based risk score in immunotherapy responses was assessed using a number of methods. Firstly, TMB acted as a biomarker of immunotherapy response (27). In patients with HCC, the low-risk score group had a higher TMB score compared with the high-risk score group (Fig. 4A; P<0.001). In addition, the immunophenoscore acted as a predictor of the response to checkpoint blockade. Patients with HCC that had a low-risk score demonstrated a higher programmed cell death protein 1 (PD-1) immunophenoscore and cytotoxic T-lymphocyte-associated protein 4 (CTLA4) immunophenoscore (Fig. 4B; all P<0.05). Moreover, low-risk score patients with HCC had a lower immune escape score (Fig. 4C; P=0.02). Furthermore, TIDE scores can predict responses to cancer immunotherapy (28). As shown in Fig. 4D, patients with HCC that had a low-risk score demonstrated a lower T cell dysfunction score, T cell exclusion score and TIDE score (all P<0.05). Additionally, HLA serves a vital role in antigen processing and antitumor immunity (29), with a high risk score indicating a higher level of HLA-related genes (Fig. 4E). Immunological checkpoints are essential in promoting self-tolerance and stifling immunological responses in malignancy.

Patients with HCC that had a low-risk score in the present study demonstrated higher levels of major immunological checkpoints (Fig. 4F; all P<0.05). These data suggested that patients with HCC that had a low-risk score would be more responsive to immunotherapy. Additionally, two immunotherapy cohorts were used to demonstrate the aforementioned findings. In patients that received immunotherapy, non-responders had a higher risk score (Fig. 4G), with this high-risk score indicating a poor OS rate (Fig. 4G). Additionally, there was a notably decreased response rate in patients with a high-risk score (Fig. 4G). The IMvigor210 cohort also showed similar outcomes (Fig. 4H). The IC_{50} value of common medications used in targeted therapy and chemotherapy for HCC was also explored. Findings indicated that patients with high-risk scores for HCC had lower IC_{50} values for chemotherapy drugs, such as 5-fluorouracil, camptothecin, docetaxel, oxaliplatin and paclitaxel and targeted therapy drugs, such as afatinib, crizotinib, dasatinib, erlotinib and osimertinib (Fig. 5A and B). Consequently, patients with HCC and a high-risk score may respond more favorably to targeted therapy and chemotherapy.

Distinct differences in cancer-related hallmarks in different GRS-based risk score groups. In order to investigate the molecular mechanisms in patients with HCC with varying GRS scores, GSEA was performed. Gene set score was associated with angiogenesis, DNA repair, epithelial mesenchymal transition (EMT) signaling, glycolysis, hypoxia, IL2-STAT5 signaling, mTORC1 signaling and the p53 pathway, and were all higher in patients with high-risk HCC (Fig. 6A-I). Patients with HCC that had a high-risk score indicated a higher apoptosis gene set score (Fig. 6J). This suggests that these biological processes may be crucial in the initiation and progression of HCC tumors.

Biological functions of MCT1 in HCC. MCT1, the gene with the maximum coefficient in the risk score calculation formula for further analysis, was selected. As shown in Fig. 7A, MCT1 was upregulated in HCC cell lines, including MHCC97, HCCLM3 and SNU449, compared with the normal liver cell line, THLE-2. Subsequently, MCT1 was knocked down in MHCC97H cell lines (Fig. 7B). EMT-related proteins were also detected, and the results indicated that downregulation of MCT1 inhibited EMT in MHCC97H cell line (Fig. 7C). The results showed that the downregulation of MCT1 inhibited colony formation in HCC and resulted in cell cycle arrest and apoptosis (Fig. 7D-F). Moreover, downregulation of MCT1 inhibited the migration and invasion of MHCC97H cell line (Fig. 7G and H).

Discussion

In the present study, a GRS was established by integrating 10 machine learning algorithms, and its prognostic value was evaluated across three independent cohorts. Among these, the model constructed using the LASSO method demonstrated a superior performance and was selected as the optimal

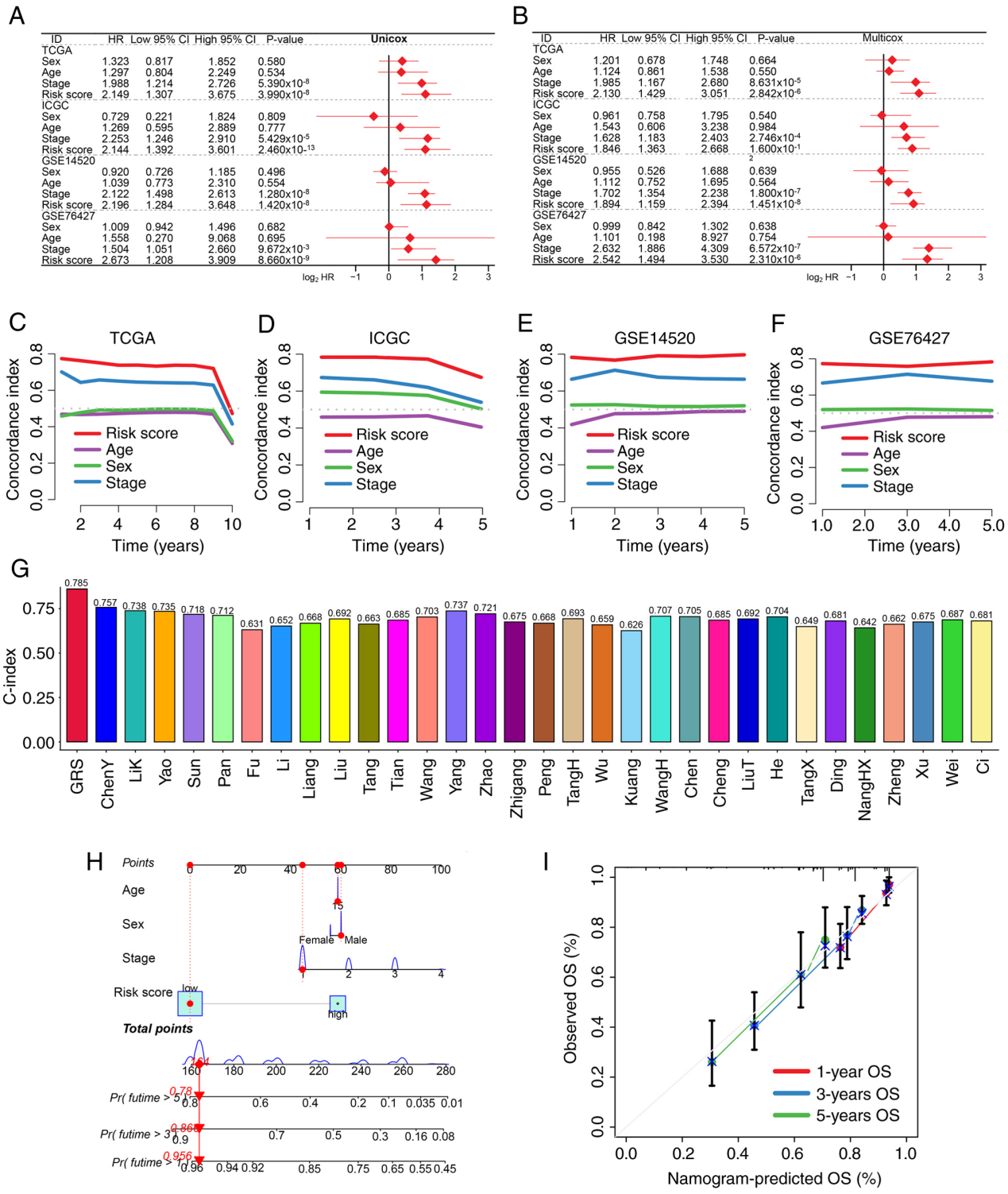

Figure 2. Assessment of the predictive performance of the GRS. (A) Univariate and (B) multivariate Cox regression analyses identified risk factors associated with HCC prognosis. C-index curves comparing GRS with clinical parameters across (C) TCGA, (D) ICGC, (E) GSE14520 and (F) GSE76427 training and testing datasets. (G) Comparison of C-index values between GRS and previously published HCC prognostic models. (H) Prognostic nomogram integrating age, sex, clinical stage and GRS score. (I) Calibration plots showing agreement between predicted and actual 1, 3 and 5-year survival probabilities. GRS, glycolysis-related signature; HCC, hepatocellular carcinoma; TCGA, The Cancer Genome Atlas; ICGC, International Cancer Genome Consortium; HR, hazard ratio; OS, overall survival.

prognostic tool. Patients with elevated GRS scores exhibited notably worse clinical outcomes, as reflected by 1, 3 and 5-year AUCs of 0.777, 0.787 and 0.766, respectively. In addition to the prognostic value, the GRS also proved effective in predicting therapeutic responsiveness in HCC.

The final GRS was comprised of seven GRGs: TCOF1, RFC4, RAE1, KIF2C, DEPDC1, ADNP and MCT1. TCOF1 has been reported to drive tumorigenesis by regulating ribosomal RNA synthesis and promoting oncogenic pathways (30). RFC4 acts as a powerful prognostic indicator and serves a role

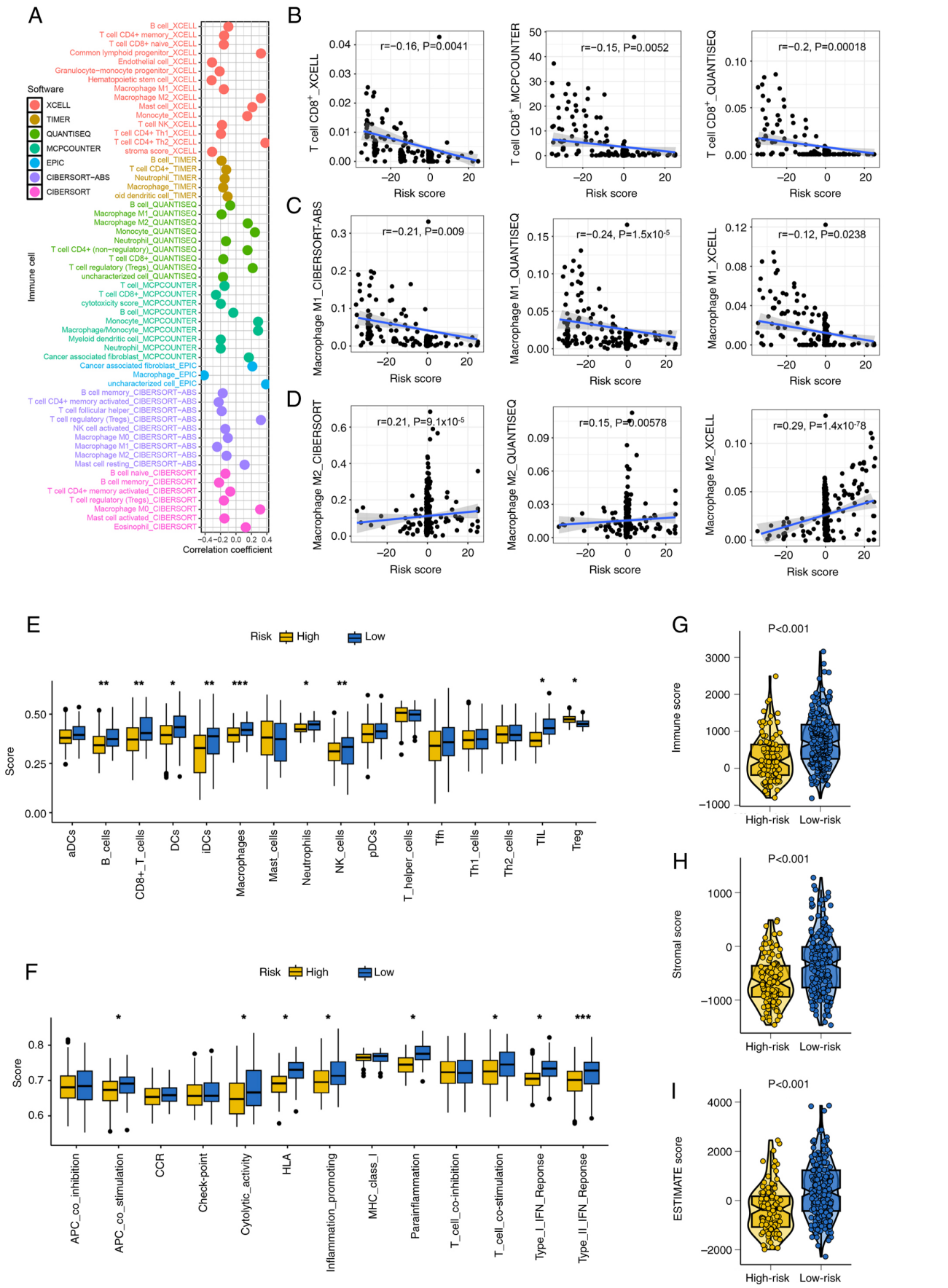

Figure 3. Tumor immune microenvironment characteristics based on the GRS. (A) Correlation between GRS and immune cell infiltration assessed by multiple deconvolution algorithms. Differential levels of (B) $CD8^+$ T cells, (C) M1 macrophages and (D) M2 macrophages across GRS subgroups. (E) Distribution of immune cell types and (F) immune-related functional pathways based on single sample gene set enrichment analysis. (G) Immune score, (H) stromal score and (I) ESTIMATE scores were significantly elevated in the low-risk group compared with the high-risk group. *P<0.05, **P<0.01 and ***P<0.001. GRS, glycolysis-related signature; ESTIMATE, estimation of stromal and immune cells in malignant tumors.

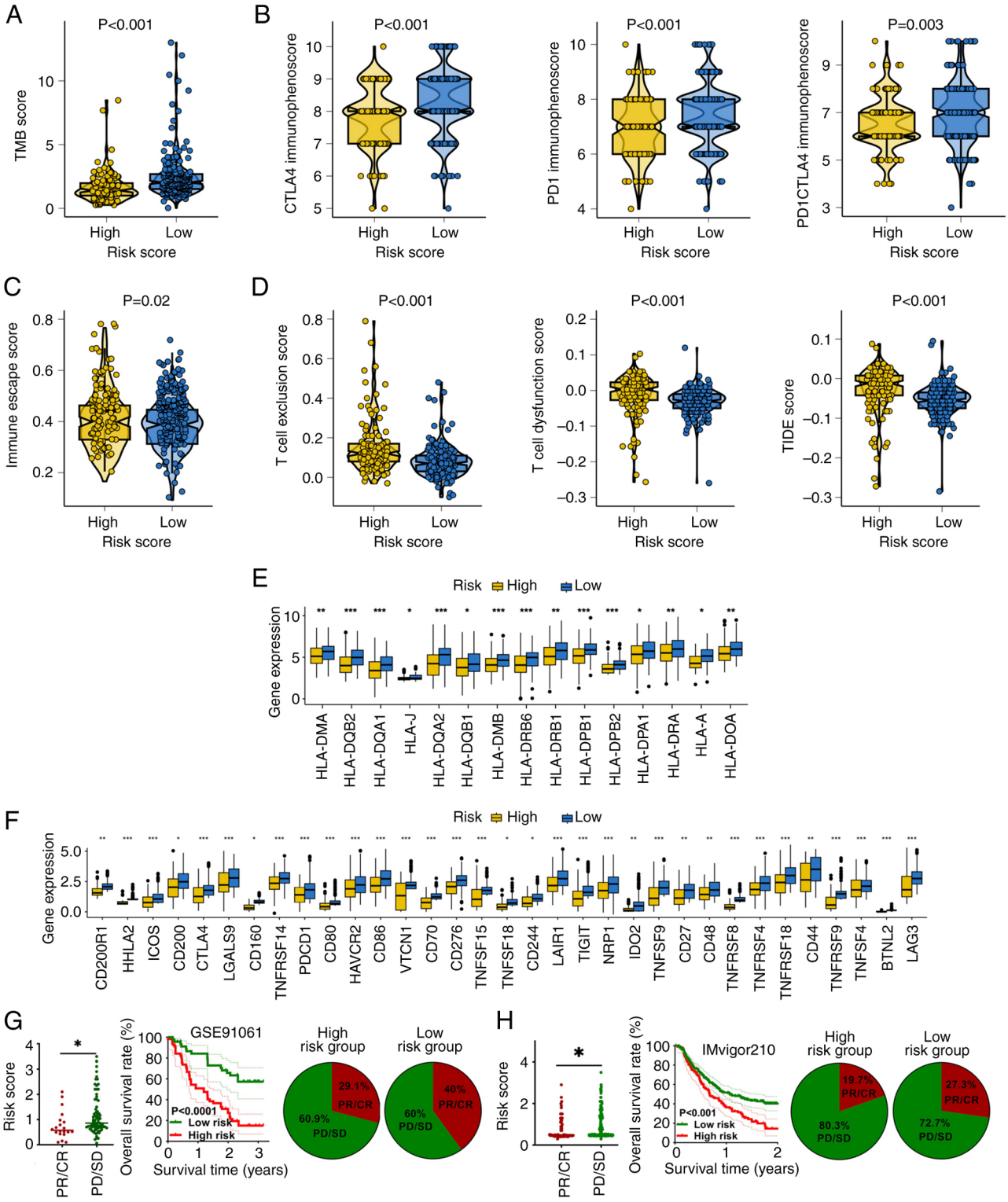

Figure 4. Predictive role of the GRS in immunotherapy responses among patients with hepatocellular carcinoma. (A) TMB and (B) immunophenoscore distributions between high and low-GRS groups. (C and D) Differences in immune escape metrics including TIDE, T cell dysfunction and exclusion scores. (E) Expression levels of HLA-associated genes and (F) immune checkpoint molecules across risk groups. Immunotherapy response rate and survival outcomes in (G) GSE91061 and (H) IMvigor210 cohorts stratified by GRS. *P<0.05, **P<0.01 and ***P<0.001. GRS, glycolysis-related signature; TMB, tumor mutational burden; HLA, human leukocyte antigen; TIDE, Tumor Immune Dysfunction and Exclusion; CTLA, cytotoxic T-lymphocyte associated protein 4; CR, complete response; PR; partial response; SD, stable disease; PD, progressive disease.

in cell proliferation within HCC (31). Moreover, RFC4 serves as a novel biomarker in pan-cancer due to its association with immune infiltration and drug response (32). A previous study also demonstrated that RAE1 was a prognostic marker for HCC and showed an association with clinicopathological characteristics (33). In addition, the silencing of KIF2C has been shown to enhance chemosensitivity through the PI3K/AKT/MAPK axis (34), and DEPDC1 promotes proliferation, invasion

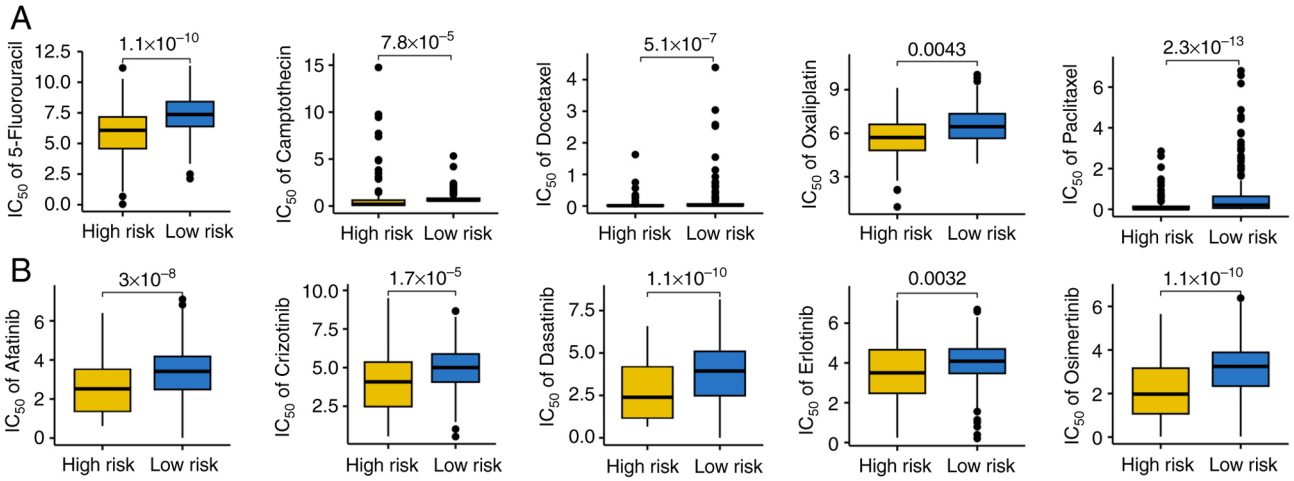

Figure 5. GRS-associated differences in drug sensitivity profiles. Estimated IC_{50} values of commonly used (A) chemotherapeutic and (B) targeted agents in high-risk vs. low-risk hepatocellular carcinoma groups, revealing enhanced sensitivity in patients with high-GRS. GRS, glycolysis-related signature.

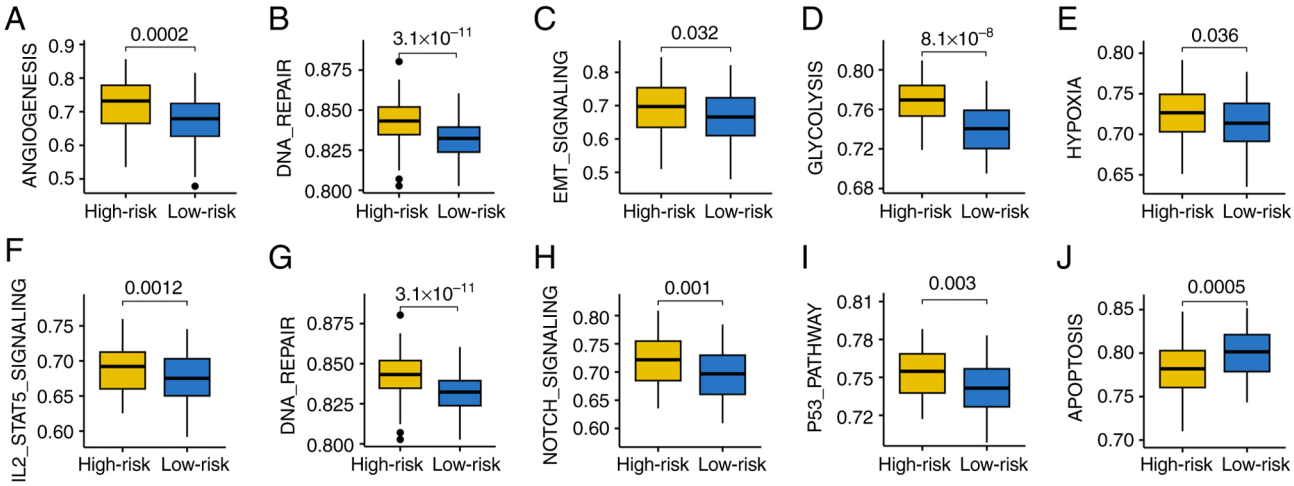

Figure 6. Enrichment of oncogenic pathways in patients with high-GRS hepatocellular carcinoma. Pathway scores for (A) angiogenesis, (B) DNA repair, (C) EMT, (D) glycolysis, (E) hypoxia, (F) IL2-STAT5 signaling, (G) mTORC1 signaling, (H) Notch signaling and (I) the p53 pathway were elevated in high-risk individuals. (J) Apoptosis-related gene set activity also increased in the high-GRS subgroup. GRS, glycolysis-related signature; EMT, epithelial mesenchymal transition.

and angiogenesis in HCC through the C-C motif chemokine ligand 20/C-C motif chemokine receptor 6 pathway (35,36). Furthermore, ADNP is linked to both immune modulation and radiosensitivity in liver cancer (37). Finally, MCT1, a key glycolytic transporter, has been implicated in autophagy-mediated metastasis and metabolic reprogramming through activation of the Wnt/β-catenin pathway (38).

Immunotherapy is a promising treatment alternative for patients who are unable to undergo surgery (39). However, reliable biomarkers that predict immunotherapy responses remain limited. The efficacy of GRS in predicting the benefits a patient may receive from immunotherapy was examined in the present study, with findings indicating that the GRS may offer predictive value in this context. Patients with HCC and higher TIDE scores, indicative of immune evasion, benefited less from immunotherapy (40), with an improved immunotherapy benefit being indicated by a higher TMB score (41). In patients with HCC that had a low-risk score, a higher TMB score as well as lower TIDE and tumor escape scores were observed. The immunophenoscore was established to forecast patient reactions to immune checkpoint inhibitor therapies, mainly using TCGA RNA-sequencing data (42). A higher immunophenoscore supports the concept that immunotherapy is more effective in patients with HCC and a low-risk score, which was in line with the findings of the present study. A worse response to immunotherapy may therefore be indicated by a higher GRS-based risk score in HCC.

The potential mechanisms underlying the association between patients with HCC with a high GRS score and poor immunotherapy benefits must be further explored. Notably, the findings of the present study align with prior studies by Zhang *et al* (43) and Peng *et al* (44), which systematically outlined the role of altered glycolysis in mediating drug resistance across diverse cancer types and other disease. Zhang *et al* (43) found that the N6-methyladenosine demethylase fat mass and obesity-associated protein (FTO) attenuates cardiac dysfunction by regulating glucose uptake

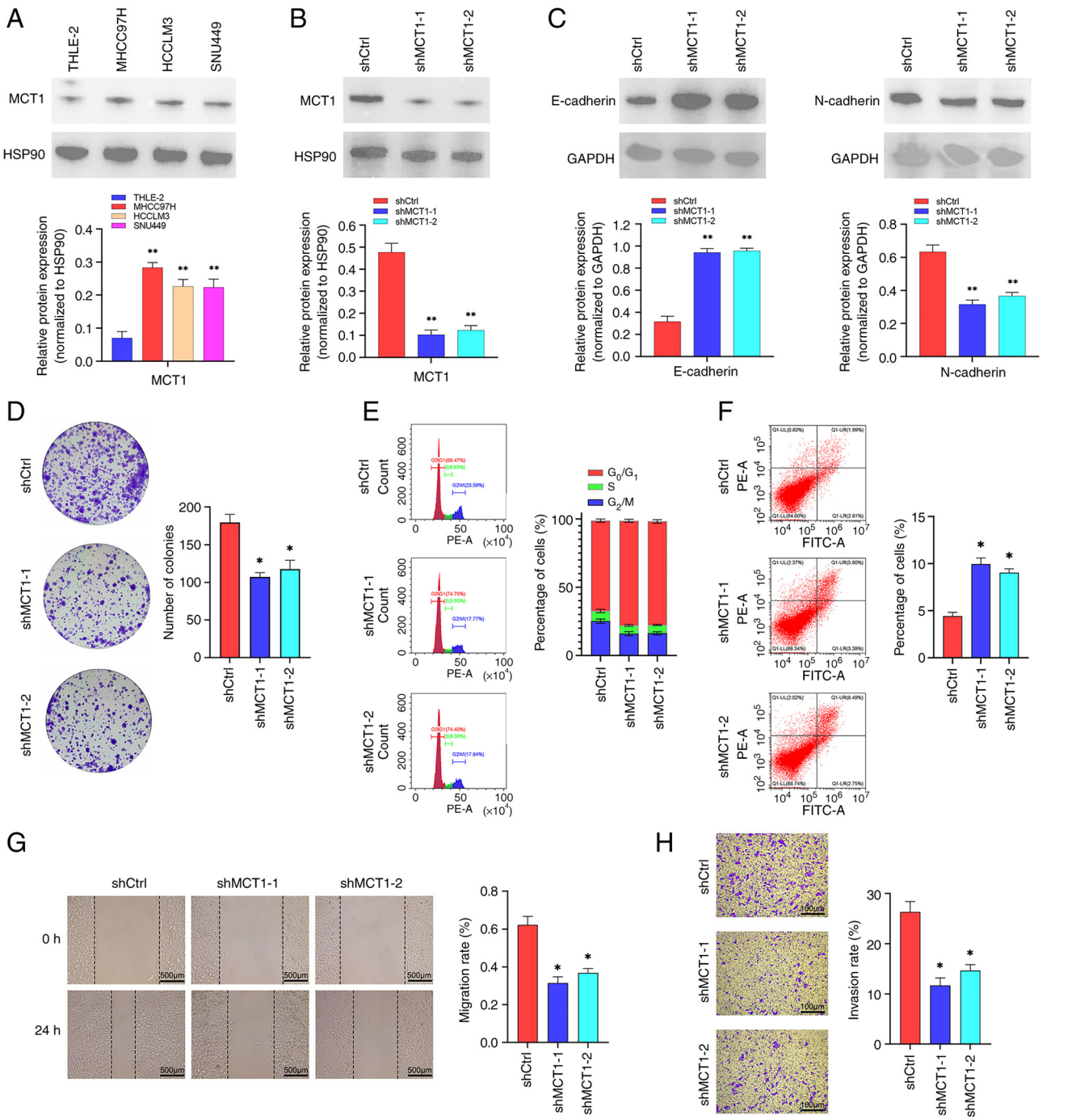

Figure 7. Biological functions of MCT1 in HCC. (A) Western blotting was applied to detect MCT1 expression levels in normal hepatic and HCC cell lines. (B) Western blotting was applied to detect MCT1 knockdown efficiency in MHCC97H cells. (C) Western blotting was applied to detect EMT-related proteins expression levels, including E-cadherin and N-cadherin protein. (D) Colony formation assay showed colony formation was impaired following MCT1 silencing. Flow cytometry showed reduced MCT1 expression caused (E) cell cycle arrest and (F) increased apoptosis. (G) Cell migratory detected by wound healing assay and (H) invasive capacities detected by Transwell assay were diminished upon MCT1 downregulation. *P<0.05 and **P<0.01. MCT1, monocarboxylic acid transporter 1; HCC, hepatocellular carcinoma; E-cadherin, epithelial cadherin; N-cadherin, neural cadherin; sh, short hairpin; Ctrl; control; ns, not significant.

and glycolysis in mice with pressure overload-induced heart failure, suggesting FTO is a potential target for heart failure prevention and treatment. Peng *et al* (44) suggested that glycolysis-driven suppression of IFN-γ signaling may contribute to immunotherapy resistance. By contrast, excessive glycolytic activity driven by STAT5-induced lactate production may also sensitize certain tumors to a PD-1/programmed death-ligand 1 (PD-L1) blockade, indicating a complex relationship between metabolic status and immune response (45). These studies emphasized that excessive lactate production and acidification of the TME impairs drug delivery and fosters immune evasion, both of which contribute to reduced therapeutic efficacy.

In the present study, high-risk patients demonstrated elevated glycolytic activity and upregulation of MCT1, a monocarboxylate transporter responsible for lactate export,

supporting the hypothesis that glycolysis-driven acidosis may underlie poor immunotherapy and chemotherapy responses. The upregulation of glycolytic genes and enrichment of pathways such as EMT, mTORC1 and hypoxia signaling in high-risk HCC, further reinforces the mechanistic links between metabolic reprogramming and treatment resistance. These observations underscore the translational potential of combining glycolysis inhibitors, such as MCT1 antagonists, with existing therapeutic regimens to overcome resistance and improve outcomes in HCC.

Functional enrichment analysis further demonstrated that several oncogenic pathways, including angiogenesis, glycolysis, hypoxia, mTORC1, EMT and p53 signaling, were upregulated in patients with a high-risk score. These biological programs promote tumor development, immune evasion and treatment resistance in HCC. Angiogenesis is important in the development of HCC (46) and hypoxia is associated with innate immunity and tumor progression in HCC (47). In addition, glycolysis is notably associated with the prognosis of HCC (48) and phenylalanyl-tRNA synthetase subunit β has been shown to promote tumor progression by activating the mTORC1 signaling pathway (49).

Notably, HCC progression may also be associated with therapeutic resistance. EMT is a mechanism in which E-cadherin expression is lost during tumor progression (50). E-cadherins are crucial cell-cell adhesion proteins with tumor suppression properties (51). Loss of E-cadherin during EMT is associated with tumor progression and broad-spectrum treatment resistance. In multiple cancers, EMT programs, occasionally precipitated or reinforced during exposure to cytotoxic agents such as cisplatin or paclitaxel, are associated with reduced drug sensitivity and increased survival of motile, detached cells (52). Recent structural and single-molecule work by Xie *et al* (53) identified 66E8, a conformation-specific monoclonal antibody against E-cadherin that stabilizes the adhesive strand-swap dimer of E-cadherin by strengthening electrostatic contacts around the N-terminal swapped β-strand and its hydrophobic pocket, thereby impeding conformational changes that favor dimer dissociation under force (53). The 'swapped β-strand' refers to the N-terminal β-strand in the extracellular cadherin domain 1 that exchanges between two E-cadherin protomers to form the strand-swap dimer, the high-affinity adhesive state that underpins epithelial cell-cell junctions. Functionally, stabilizing cadherin-mediated adhesion is expected to reduce detachment and anoikis resistance, blunt EMT-like migratory programs and re-sensitize tumors to therapy by restoring mechanotransduction and immune engagement at tumor-immune interfaces. Complementing this, pro-inflammatory IL-17A can downregulate E-cadherin and upregulate PD-L1, fostering immune evasion (54). Thus, therapeutic angles for future studies in HCC include: i) Adhesion-stabilizing biologics (such as 66E8 or E-cadherin-stabilizing peptides) to curb dissemination and enhance chemotherapy efficacy; ii) combination strategies pairing adhesion stabilization with immune checkpoint blockade to counter IL-17A-driven PD-L1 induction; and iii) rational combinations with metabolic modulators (such as inhibitors targeting glycolysis/MCT1 in GRS-high, EMT-enriched tumors) to simultaneously relieve acidosis-driven EMT and reinforce junctional adhesion. Collectively, these approaches support the concept that enhancing E-cadherin adhesion may inhibit HCC progression and improve therapeutic benefits.

There are several limitations of the present study which must be acknowledged. Firstly, although the expression and function of MCT1 was evaluated *in vitro*, *in vivo* experiments are required to demonstrate its role in tumor progression. Secondly, the analyses were primarily based on transcriptomic data, which may not fully capture protein-level or functional dynamics. Lastly, external validation within an in-house or prospective cohort would further strengthen the generalizability of the findings of the present study.

In conclusion, the present study developed a novel GRS for HCC, serving as an indicator for predicting clinical outcomes and immunotherapeutic responses.

Acknowledgements

Not applicable.

Funding

This study was supported by grants from the Hunan Provincial Natural Science Foundation (grant nos. 2023JJ40387 and 2024JJ6276), Hunan Provincial Key Field Research and Development Program (grant no. 2022SK2162) and the Natural Science Foundation of Changsha (grant no. kq2208120).

Availability of data and materials

The data generated in the present study may be requested from the corresponding authors.

Authors' contributions

YZ contributed to writing, original draft preparation, bioinformatics analysis and experimental research. WL contributed to writing and conceptualization and methodology. ZF contributed to the writing, software used and data collection. KZ contributed to methodology and visualization. XH contributed to conception, writing, reviewing and editing. SL contributed to the software used and acquisition of data. WZ and QW were involved in validation and analysis of data. XC and ZX contributed to study design and supervision. YZ and WL confirm the authenticity of all the raw data. All authors read and approved the final version of the manuscript.

Ethics approval and consent to participate

Not applicable.

Patient consent for publication

Not applicable.

Competing interests

The authors declare that they have no competing interests.

References

1. Vogel A, Meyer T, Sapisochin G, Salem R and Saborowski A: Hepatocellular carcinoma. Lancet 400: 1345-1362, 2022.
2. Sung H, Ferlay J, Siegel RL, Laversanne M, Soerjomataram I, Jemal A and Bray F: Global cancer statistics 2020: GLOBOCAN estimates of incidence and mortality worldwide for 36 cancers in 185 countries. CA Cancer J Clin 71: 209-249, 2021.
3. Chidambaranathan-Reghupaty S, Fisher PB and Sarkar D: Hepatocellular carcinoma (HCC): Epidemiology, etiology and molecular classification. Adv Cancer Res 149: 1-61, 2021.
4. Wang Y, Yang Y, Zhao Z, Sun H, Luo D, Huttad L, Zhang B and Han B: A new nomogram model for prognosis of hepatocellular carcinoma based on novel gene signature that regulates cross-talk between immune and tumor cells. BMC Cancer 22: 379, 2022.
5. Hanahan D and Weinberg RA: Hallmarks of cancer: The next generation. Cell 144: 646-674, 2011.
6. Icard P, Shulman S, Farhat D, Steyaert JM, Alifano M and Lincet H: How the Warburg effect supports aggressiveness and drug resistance of cancer cells? Drug Resist Updat 38: 1-11, 2018.
7. Hanahan D: Hallmarks of cancer: New dimensions. Cancer Discov 12: 31-46, 2022.
8. Han X, Ren C, Yang T, Qiao P, Wang L, Jiang A, Meng Y, Liu Z, Du Y and Yu Z: Negative regulation of AMPKα1 by PIM2 promotes aerobic glycolysis and tumorigenesis in endometrial cancer. Oncogene 38: 6537-6549, 2019.
9. Zhang D, Tang Z, Huang H, Zhou G, Cui C, Weng Y, Liu W, Kim S, Lee S, Perez-Neut M, *et al*: Metabolic regulation of gene expression by histone lactylation. Nature 574: 575-580, 2019.
10. Huang H, Chen K, Zhu Y, Hu Z, Wang Y, Chen J, Li Y, Li D and Wei P: A multi-dimensional approach to unravel the intricacies of lactylation related signature for prognostic and therapeutic insight in colorectal cancer. J Transl Med 22: 211, 2024.
11. Huang R, Li Y, Lin K, Zheng L, Zhu X, Huang L and Ma Y: A novel glycolysis-related gene signature for predicting prognosis and immunotherapy efficacy in breast cancer. Front Immunol 16: 1512859, 2025.
12. Shen C, Suo Y, Guo J, Su W, Zhang Z, Yang S, Wu Z, Fan Z, Zhou X and Hu H: Development and validation of a glycolysis-associated gene signature for predicting the prognosis, immune landscape, and drug sensitivity in bladder cancer. Front Immunol 15: 1430583, 2024.
13. Xu Q, Miao D, Song X, Chen Z, Zeng L, Zhao L, Xu J, Lin Z and Yu F: Glycolysis-related gene signature can predict survival and immune status of hepatocellular carcinoma. Ann Surg Oncol 29: 3963-3976, 2022.
14. Grinchuk OV, Yenamandra SP, Iyer R, Singh M, Lee HK, Lim KH, Chow PK and Kuznetsov VA: Tumor-adjacent tissue co-expression profile analysis reveals pro-oncogenic ribosomal gene signature for prognosis of resectable hepatocellular carcinoma. Mol Oncol 12: 89-113, 2018.
15. Roessler S, Jia HL, Budhu A, Forgues M, Ye QH, Lee JS, Thorgeirsson SS, Sun Z, Tang ZY, Qin LX and Wang XW: A unique metastasis gene signature enables prediction of tumor relapse in early-stage hepatocellular carcinoma patients. Cancer Res 70: 10202-10212, 2010.
16. Riaz N, Havel JJ, Makarov V, Desrichard A, Urba WJ, Sims JS, Hodi FS, Martín-Algarra S, Mandal R, Sharfman WH, *et al*: Tumor and microenvironment evolution during immunotherapy with nivolumab. Cell 171: 934-949.e16, 2017.
17. Rosenberg JE, Galsky MD, Powles T, Petrylak DP, Bellmunt J, Loriot Y, Necchi A, Hoffman-Censits J, Perez-Gracia JL, van der Heijden MS, *et al*: Atezolizumab monotherapy for metastatic urothelial carcinoma: Final analysis from the phase II IMvigor210 trial. ESMO Open 9: 103972, 2024.
18. Cheng Z, Huang H, Li M, Liang X, Tan Y and Chen Y: Lactylation-related gene signature effectively predicts prognosis and treatment responsiveness in hepatocellular carcinoma. Pharmaceuticals (Basel) 16: 644, 2023.
19. Yang X, Li X, Cheng Y, Zhou J, Shen B, Zhao L and Wang J: Comprehensive analysis of the glycolysis-related gene prognostic signature and immune infiltration in endometrial cancer. Front Cell Dev Biol 9: 797826, 2022.
20. Zhang X, Li Y and Chen Y: Development of a comprehensive gene signature linking hypoxia, glycolysis, lactylation, and metabolomic insights in gastric cancer through the integration of bulk and single-cell RNA-Seq data. Biomedicines 11: 2948, 2023.
21. Ritchie ME, Phipson B, Wu D, Hu Y, Law CW, Shi W and Smyth GK: limma powers differential expression analyses for RNA-sequencing and microarray studies. Nucleic Acids Res 43: e47, 2015.
22. Liu Z, Liu L, Weng S, Guo C, Dang Q, Xu H, Wang L, Lu T, Zhang Y, Sun Z and Han X: Machine learning-based integration develops an immune-derived lncRNA signature for improving outcomes in colorectal cancer. Nat Commun 13: 816, 2022.
23. Yoshihara K, Shahmoradgoli M, Martínez E, Vegesna R, Kim H, Torres-Garcia W, Treviño V, Shen H, Laird PW, Levine DA, *et al*: Inferring tumour purity and stromal and immune cell admixture from expression data. Nat Commun 4: 2612, 2013.
24. Sturm G, Finotello F and List M: Immunedeconv: An R package for unified access to computational methods for estimating immune cell fractions from bulk RNA-sequencing data. Methods Mol Biol 2120: 223-232, 2020.
25. Hänzelmann S, Castelo R and Guinney J: GSVA: Gene set variation analysis for microarray and RNA-seq data. BMC Bioinformatics 14: 7, 2013.
26. Maeser D, Gruener RF and Huang RS: oncoPredict: an R package for predicting in vivo or cancer patient drug response and biomarkers from cell line screening data. Brief Bioinform 22: bbab260, 2021.
27. Ansari A, Ray SK, Sharma M, Rawal R and Singh P: Tumor mutational burden as a biomarker of immunotherapy response: An immunogram approach in onco-immunology. Curr Mol Med 24: 1461-1469, 2024.
28. Jiang P, Gu S, Pan D, Fu J, Sahu A, Hu X, Li Z, Traugh N, Bu X, Li B, *et al*: Signatures of T cell dysfunction and exclusion predict cancer immunotherapy response. Nat Med 24: 1550-1558, 2018.
29. Maggs L, Sadagopan A, Moghaddam AS and Ferrone S: HLA class I antigen processing machinery defects in antitumor immunity and immunotherapy. Trends Cancer 7: 1089-1101, 2021.
30. Wu C, Xia D, Wang D, Wang S, Sun Z, Xu B and Zhang D: TCOF1 coordinates oncogenic activation and rRNA production and promotes tumorigenesis in HCC. Cancer Sci 113: 553-564, 2022.
31. Chen P, Liu Y, Ma X, Li Q, Zhang Y, Xiong Q and Song T: Replication factor C4 in human hepatocellular carcinoma: A potent prognostic factor associated with cell proliferation. Biosci Trends 15: 249-256, 2021.
32. Yu L, Li J, Zhang M, Li Y, Bai J, Liu P, Yan J and Wang C: Identification of RFC4 as a potential biomarker for pan-cancer involving prognosis, tumour immune microenvironment and drugs. J Cell Mol Med 28: e18478, 2024.
33. Chi G, Pei JH and Li XQ: RAE1 is a prognostic biomarker and is correlated with clinicopathological characteristics of patients with hepatocellular carcinoma. BMC Bioinformatics 23: 252, 2022.
34. Wei S, Lu C, Mo S, Huang H, Chen M, Li S, Kong L, Zhang H, Hoa PTT, Han C and Luo X: Silencing of KIF2C enhances the sensitivity of hepatocellular carcinoma cells to cisplatin through regulating the PI3K/AKT/MAPK signaling pathway. Anticancer Drugs 35: 237-250, 2024.
35. Amisaki M, Yagyu T, Uchinaka EI, Morimoto M, Hanaki T, Watanabe J, Tokuyasu N, Sakamoto T, Honjo S and Fujiwara Y: Prognostic value of DEPDC1 expression in tumor and non-tumor tissue of patients with hepatocellular carcinoma. Anticancer Res 39: 4423-4430, 2019.
36. Guo W, Li H, Liu H, Ma X, Yang S and Wang Z: DEPDC1 drives hepatocellular carcinoma cell proliferation, invasion and angiogenesis by regulating the CCL20/CCR6 signaling pathway. Oncol Rep 42: 1075-1089, 2019.
37. Wang X, Peng H, Zhang G, Li Z, Du Z, Peng B and Cao P: ADNP is associated with immune infiltration and radiosensitivity in hepatocellular carcinoma for predicting the prognosis. BMC Med Genomics 16: 178, 2023.
38. Fan Q, Yang L, Zhang X, Ma Y, Li Y, Dong L, Zong Z, Hua X, Su D, Li H and Liu J: Autophagy promotes metastasis and glycolysis by upregulating MCT1 expression and Wnt/β-catenin signaling pathway activation in hepatocellular carcinoma cells. J Exp Clin Cancer Res 37: 9, 2018.
39. Riley RS, June CH, Langer R and Mitchell MJ: Delivery technologies for cancer immunotherapy. Nat Rev Drug Discov 18: 175-196, 2019.
40. Fu J, Li K, Zhang W, Wan C, Zhang J, Jiang P and Liu XS: Large-scale public data reuse to model immunotherapy response and resistance. Genome Med 12: 21, 2020.

41. Liu L, Bai X, Wang J, Tang XR, Wu DH, Du SS, Du XJ, Zhang YW, Zhu HB, Fang Y, *et al*: Combination of TMB and CNA stratifies prognostic and predictive responses to immunotherapy across metastatic cancer. Clin Cancer Res 25: 7413-7423, 2019.
42. Zanfardino M, Pane K, Mirabelli P, Salvatore M and Franzese M: TCGA-TCIA impact on radiogenomics cancer research: A systematic review. Int J Mol Sci 20: 6033, 2019.
43. Zhang B, Jiang H, Wu J, Cai Y, Dong Z, Zhao Y, Hu Q, Hu K, Sun A and Ge J: m6A demethylase FTO attenuates cardiac dysfunction by regulating glucose uptake and glycolysis in mice with pressure overload-induced heart failure. Signal Transduct Target Ther 6: 377, 2021.
44. Peng J, Cui Y, Xu S, Wu X, Huang Y, Zhou W, Wang S, Fu Z and Xie H: Altered glycolysis results in drug-resistant in clinical tumor therapy. Oncol Lett 21: 369, 2021.
45. Huang ZW, Zhang XN, Zhang L, Liu LL, Zhang JW, Sun YX, Xu JQ, Liu Q and Long ZJ: STAT5 promotes PD-L1 expression by facilitating histone lactylation to drive immunosuppression in acute myeloid leukemia. Signal Transduct Target Ther 8: 391, 2023.
46. Zhang F, Wang B, Zhang W, Xu Y, Zhang C and Xue X: Transcription factor MAZ potentiates the upregulated NEIL3-mediated aerobic glycolysis, thereby promoting angiogenesis in hepatocellular carcinoma. Curr Cancer Drug Targets 24: 1235-1249, 2024.
47. Yuen VW and Wong CC: Hypoxia-inducible factors and innate immunity in liver cancer. J Clin Invest 130: 5052-5062, 2020.
48. Wang B and Pu R: Association between glycolysis markers and prognosis of liver cancer: A systematic review and meta-analysis. World J Surg Oncol 21: 390, 2023.
49. Wang Y, Wang G, Hu S, Yin C, Zhao P, Zhou X, Shao S, Liu R, Hu W, Liu GL, *et al*: FARSB facilitates hepatocellular carcinoma progression by activating the mTORC1 signaling pathway. Int J Mol Sci 24: 16709, 2023.
50. Kaszak I, Witkowska-Piłaszewicz O, Niewiadomska Z, Dworecka-Kaszak B, Ngosa Toka F and Jurka P: Role of cadherins in cancer-a review. Int J Mol Sci 21: 7624, 2020.
51. Lee G, Wong C, Cho A, West JJ, Crawford AJ, Russo GC, Si BR, Kim J, Hoffner L, Jang C, *et al*: E-cadherin induces serine synthesis to support progression and metastasis of breast cancer. Cancer Res 84: 2820-2835, 2024.
52. Hashemi M, Arani HZ, Orouei S, Fallah S, Ghorbani A, Khaledabadi M, Kakavand A, Tavakolpournegari A, Saebfar H, Heidari H, *et al*: EMT mechanism in breast cancer metastasis and drug resistance: Revisiting molecular interactions and biological functions. Biomed Pharmacother 155: 113774, 2022.
53. Xie B, Xu S, Schecterson L, Gumbiner BM and Sivasankar S: Strengthening E-cadherin adhesion via antibody-mediated binding Structure 32: 217-227.e3, 2024.
54. Liao H, Chang X, Gao L, Ye C, Qiao Y, Xie L, Lin J, Cai S and Dong H: IL-17A promotes tumorigenesis and upregulates PD-L1 expression in non-small cell lung cancer. J Transl Med 21: 828, 2023.